Dynamic Modeling and Control of Parallel Robots With Elastic Cables: Singular Perturbation Approach

Mohammad A. Khosravi, *Member, IEEE*, and Hamid D. Taghirad, *Senior Member, IEEE*

***Abstract*—In this paper, control of fully–constrained parallel cable robots with elastic cables is studied in detail. In the modeling process, longitudinal vibration of cables is considered as their dominant dynamics, and the governing equations of motion are rewritten to the standard form of singular perturbation. The proposed composite controller consists of two main components. A rigid controller is designed based on the slow or rigid model of the system and a corrective term is added to guarantee asymptotic stability of the fast dynamics. Then, by using Tikhonov theorem, slow and fast variables are separated and incorporated into the stability analysis of the overall closed–loop system, and a set of sufficient conditions for the stability of the total system is derived. Finally, the effectiveness of the proposed control law is verified through simulations.**

***Index Terms*—Cable driven parallel robots, composite control, elastic cable, Lyapunov analysis, singular perturbation, stability analysis, Tikhonov theorem.**

I. Introduction

SINCE the late 1980s, the study of cable driven parallel robots has received increasing attention. By replacing the rigid links in parallel robots with cables, some of the traditional shortcomings of conventional robots are remedied. Using cables instead of rigid links introduces many potential applications such as very large workspace robots [1], high speed manipulation [2], handling of heavy materials [3], cleanup of disaster areas [4], access to remote locations, and interaction with hazardous environments [5]. Cable robots can be sorted into two types: fully–constrained and under–constrained manipulators [4], [6], [7]. In the fully–constrained robots, cables can create any wrench on the end–effector [8] or equivalently, for a given set of cable lengths, the end–effector cannot be moved in position and orientation [9]. The cable robots under study in this paper are restricted to the fully-constrained type and it is assumed that the motion control is performed just in the wrench-closure workspace.

Replacing rigid links with cables introduces new challenges to the study of cable driven robots, of which control is the most critical. Cables can only apply tensile forces and they can only be used to pull and not to push an object. Therefore, in order to avoid structural failures, control algorithm should be designed such that all cables remain under tension in all configurations. Dynamic behavior of the cables is another major challenge in mechanical design and control of such robots. Cables can be modeled as elastic elements and may encounter elongation and vibration. Therefore, elasticity in cables may cause position and orientation errors for the moving platform. Furthermore, due to the axial vibrations in cables, the moving platform may experience unwanted vibrations, and even become uncontrollable. This problem is a critical concern in applications where high bandwidth or high stiffness is a stringent requirement [10]. Again, to encounter this problem, control is playing a vital role. Proposed control strategies for cable robots should be able to efficiently damp vibrations and achieve good tracking performance.

Control of cable driven robots has received limited attention compared with that of conventional robots. With the assumption of massless and inextensible models for the cable, most of the common control strategies for conventional robots have been adapted for cable robots. Lyapunov based control [2], [11], computed torque method [11], [12], sliding mode [13], robust PID control [14], and adaptive PD control [15] are some of reported control algorithms being used in the control of cable robots. Kawamura *et al.* have proposed a PD controller accompanied with gravity compensation and internal forces in the cable-length coordinates [2]. The stability of motion is analyzed based on the Lyapunov theorem and vector closure conditions. Alp and Agrawal [11] used PD control with gravity compensation in task space coordinates and analyzed asymptotic stability based on the Lyapunov second method. Inverse dynamics control (IDC) or computed torque technique is another method which is used in [11] and [12]. In this technique, the actuator forces are calculated to cancel out the effects of nonlinear dynamical terms on the manipulator. Fang *et al.* [16] used nonlinear feed forward control laws in the cable length coordinates. They proposed optimal tension distribution algorithm to compensate dynamic errors. In [17], an approach based on the Hessian matrix was developed to conduct the stability analysis of equilibrium configurations for 3-D cable systems with multiple aerial robots.

However, in these studies, cables are treated as massless inextensible strings, and no elasticity in cables are considered. It should be noted that modeling the dynamic effects of elastic cables is an extremely comprehensive task. Furthermore, it is also important to note that the obtained model must be not only sufficiently accurate, it must be usable for controller

Manuscript received May 5, 2013; revised October 6, 2013; accepted December 30, 2013. Date of publication January 22, 2014; date of current version June 3, 2014. This paper was recommended for publication by Associate Editor J. Dai and Editor C. Torras upon evaluation of the reviewers' comments. This work was supported by INSF Grant No. 87040331.

The authors are with the Advanced Robotics and Automated Systems, Industrial Control Center of Excellence, Faculty of Electrical and Computer Engineering, K.N. Toosi University of Technology, Tehran 19697, Iran (e-mail: makh@ee.kntu.ac.ir; Taghirad@kntu.ac.ir).

Color versions of one or more of the figures in this paper are available online at http://ieeexplore.ieee.org.

Digital Object Identifier 10.1109/TRO.2014.2298057

synthesis, as well. Therefore, in practice, the inclusion of only dominant effects in the dynamic analysis is proposed. For this reason, in many robotic applications, cable masses have been neglected and cable has been considered to be a nonelastic element [11], [18]. However, in practice, using this assumption will mislead the results in control especially the stability of the manipulator. Ottaviano and Castelli [19] have analyzed the effects of cable mass and elasticity and their effects on pose capability of the cable robots. They have shown that cable mass can be neglected if the ratio of the end-effector to cable masses is large or generally, the ratio of the end-effector wrenches to the cable tensions is small. Using natural frequencies of system, Diao and Ma in [10] have shown that in fully–constrained cable robots, transversal vibration of cables has very limited effects on the vibration of the end-effector and can be ignored compared with that of axial flexibility. Therefore, dominant dynamic characteristics of cable can be modeled by an axial spring in dynamic modeling of fully-constrained cable robots. According to these results, in this paper, linear axial spring is used to model dominant dynamics of the cable and by this means, a more precise model of fully-constrained cable robots is derived for the controller design and stability analysis of such robots.

Inclusion of cable dynamic characteristics in the modeling of the cable robots leads to complication in control algorithms and research on this topic is in its infancy and is very limited. Meunier *et al.* used multiloop control scheme for large adaptive reflector (LAR), in which the inner loop deals with cable model. This loop uses H_∞ controller and gain scheduling technique for adaptation of H_∞ with cable lengths. In the outer loop, a PID+IDC structure is used [20]. However, in this research, stability analysis of the closed–loop system has not been performed. In [21], elastic massless model for cable is derived and a new model for the cable robot and a new control algorithm are proposed. This control algorithm is formed in cable length space and uses internal force concept and a damping term. Stability of closed-loop system is analyzed through the Lyapunov theory and vector closure conditions.

Since both the capability of the cable robot to achieve high accuracy in positioning and its vibrations depend directly on the control scheme of the system, investigation of the control and the stability in parallel robots with elastic cables is of particular importance. However, only a few works have systematically treated these aspects. The main goal of this paper is to develop a new approach to dynamic modeling and control of cable robots with elastic cables using singular perturbation theory. With the assumption of axial spring model for the cables, singular perturbation theory is found to be very suitable for modeling and control of cable robots. Singular perturbations cause a multitime scale behavior of dynamic systems characterized by presence of both slow and fast transients in the response of the system [22]. Thus, dynamics of system can be divided into two subsystems, namely, slow and fast dynamics. These subsystems are used in the design of efficient control algorithms. The effectiveness of this theory has been investigated in modeling and control of flexible joint robots [23], but rarely in cable robots [24], [25].

The structure of this paper is as follows. First, dynamics of cable robot with ideal nonelastic cables is elaborated on and a new control algorithm is proposed for it. Then, asymptotic stability of rigid system with the proposed controller is analyzed through the Lyapunov theory. In the following sections, dynamics of cable robots with elastic cable is derived and it is rewritten to the standard form of singular perturbation. A composite control structure is proposed for this model, which consists of a rigid control term in accordance with corresponding slow or rigid model of the system and a corrective term for vibrational damping. Next, Using Tikhonov's theorem, slow and fast variables are separated and incorporated in to the stability analysis of the closed-loop system. Then, total stability of system is analyzed and sufficient conditions for its asymptotic stability are derived. Finally, to demonstrate the effectiveness of the proposed controller, simulation results on a spatial cable robot are discussed.

II. Control of Parallel Robots With Nonelastic Cables

In this section, we assume that elasticity of cables can be ignored and cables behave as massless rigid strings. This simple model has been used in many papers [11], [18]. Based on this assumption, the standard model for the overall dynamics of n-cable parallel robot with actuators is developed in [21] and [26] and given as follows:

$$\boldsymbol{M}_{eq}(\boldsymbol{x})\ddot{\boldsymbol{x}} + \boldsymbol{C}_{eq}(\boldsymbol{x},\dot{\boldsymbol{x}})\dot{\boldsymbol{x}} + \boldsymbol{G}_{eq}(\boldsymbol{x}) = \boldsymbol{J}^T(\boldsymbol{x})\boldsymbol{u}_r \tag{1}$$

in which

$$\begin{cases} \boldsymbol{M}_{eq}(\boldsymbol{x}) = r\boldsymbol{M}(\boldsymbol{x}) + r^{-1}\boldsymbol{J}^T\boldsymbol{I}_m\boldsymbol{J} \\ \boldsymbol{C}_{eq}(\boldsymbol{x},\dot{\boldsymbol{x}}) = r\boldsymbol{C}(\boldsymbol{x},\dot{\boldsymbol{x}}) + r^{-1}\boldsymbol{J}^T\boldsymbol{I}_m\dot{\boldsymbol{J}} \\ \boldsymbol{G}_{eq}(\boldsymbol{x}) = r\boldsymbol{G}(\boldsymbol{x}) \end{cases} \tag{2}$$

where $\boldsymbol{x} \in \boldsymbol{R}^6$ is the vector of generalized coordinates, $\boldsymbol{M}(\boldsymbol{x})$ is the 6×6 inertia matrix, $\boldsymbol{I}_m$ is diagonal matrix of actuator inertias reflected to the cable side of the gears, $\boldsymbol{C}(\boldsymbol{x},\dot{\boldsymbol{x}})$ represents the Coriolis and centrifugal matrix, $\boldsymbol{G}(\boldsymbol{x})$ is the gravitational terms, r is radius of pulleys, and $\boldsymbol{u}_r$ represents the input torque. $\boldsymbol{J}$ represents the Jacobian of robot and relates the derivative of generalized coordinate $\dot{\boldsymbol{x}}$, to derivative of cable length vector $\dot{\boldsymbol{L}}$ by $\dot{\boldsymbol{L}} = \boldsymbol{J}\dot{\boldsymbol{x}}$. Although these equations are nonlinear and coupled, they have inherited some properties seen in general robotic manipulators, which are very helpful in the design of control strategies.

Property 1: The inertia matrix $\boldsymbol{M}_{eq}(\boldsymbol{x})$ is symmetric and positive definite.

Property 2: The matrix $\dot{\boldsymbol{M}}_{eq}(\boldsymbol{x}) - 2\boldsymbol{C}_{eq}(\boldsymbol{x},\dot{\boldsymbol{x}})$ is skew symmetric.

A. Control Algorithm

Given a twice continuously differentiable reference trajectory $\boldsymbol{x}_d$ for (1), consider the following control law

$$\begin{aligned} \boldsymbol{u}_r = \boldsymbol{J}^\dagger(&\boldsymbol{M}_{eq}(\boldsymbol{x})\ddot{\boldsymbol{x}}_d + \boldsymbol{C}_{eq}(\boldsymbol{x},\dot{\boldsymbol{x}})\dot{\boldsymbol{x}}_d + \boldsymbol{G}_{eq}(\boldsymbol{x}) \\ &+ \boldsymbol{K}_p(\boldsymbol{x}_d - \boldsymbol{x}) + \boldsymbol{K}_v(\dot{\boldsymbol{x}}_d - \dot{\boldsymbol{x}})) + \boldsymbol{Q} \end{aligned} \tag{3}$$

where $\boldsymbol{M}_{eq}, \boldsymbol{C}_{eq}$, and $\boldsymbol{G}_{eq}$ are defined in (2) and $\boldsymbol{K}_p, \boldsymbol{K}_v$ are diagonal matrices of positive gains. $\boldsymbol{J}^\dagger$ denotes the pseudoinverse of $\boldsymbol{J}^T$, which is determined by $\boldsymbol{J}^\dagger = \boldsymbol{J}(\boldsymbol{J}^T\boldsymbol{J})^{-1}$. The

final term $\boldsymbol{Q}$, is a vector that spans the null space of $\boldsymbol{J}^T$

$$\boldsymbol{J}^T\boldsymbol{Q} = \boldsymbol{0}. \tag{4}$$

It is important to note that the vector $\boldsymbol{Q}$ does not contribute to the motion of the end-effector and only causes internal forces in the cables. This term ensures that all cables remain in tension in the whole workspace. In this paper, we assume that the motion is within the wrench–closure workspace and as a consequence, positive internal forces can be produced to keep the cables in tension.

Furthermore, it is notable that internal forces are necessary for the rigidity of the manipulator, but they can change the overall stiffness of the system [27]. If the pose of the end-effector is stabilizable, increasing the internal forces enhances the equivalent stiffness of the mechanism [28]. In the cable robots, stabilizability criterion ensures that the cable robot is stable in any circumstances as long as the internal forces are large enough [28]. In other words, when a manipulator is stabilizable in a certain pose, it can become more stiff by increasing the internal forces. Stabilizability of a cable robot depends on its geometrical parameters [29]. Based on the aforementioned facts, the equivalent stiffness of the manipulator can be controlled by the internal forces. This means that according to the end–effector pose and geometrical parameters of the manipulator, the vector of internal forces can be chosen such that the cables remain in tension, and furthermore, equivalent stiffness of the cable robot is enhanced.

B. Stability Analysis

Substitute (3) in (1) and use (4), the closed–loop system may be written as:

$$\boldsymbol{M}_{eq}(\boldsymbol{x})\ddot{\boldsymbol{e}} + \boldsymbol{C}_{eq}(\boldsymbol{x},\dot{\boldsymbol{x}})\dot{\boldsymbol{e}} + \boldsymbol{K}_p\boldsymbol{e} + \boldsymbol{K}_v\dot{\boldsymbol{e}} = \boldsymbol{0} \tag{5}$$

where

$$\boldsymbol{e} = \boldsymbol{x}_d - \boldsymbol{x}. \tag{6}$$

Consider the following Lyapunov function for the closed loop system (5)

$$V_R = \frac{1}{2}\dot{\boldsymbol{e}}^T\boldsymbol{M}_{eq}(\boldsymbol{x})\dot{\boldsymbol{e}} + \frac{1}{2}\boldsymbol{e}^T\boldsymbol{K}_p\boldsymbol{e} \tag{7}$$

which is generated using total energy in the system and it is positive, if $\boldsymbol{K}_p$ is chosen to be positive definite, since based on property 1, $\boldsymbol{M}_{eq}$ is positive definite. The time derivative of the Lyapunov function V_R is given by

$$\dot{V}_R = \dot{\boldsymbol{e}}^T\boldsymbol{M}_{eq}(\boldsymbol{x})\ddot{\boldsymbol{e}} + \boldsymbol{e}^T\boldsymbol{K}_p\dot{\boldsymbol{e}} + \frac{1}{2}\dot{\boldsymbol{e}}^T\dot{\boldsymbol{M}}_{eq}(\boldsymbol{x})\dot{\boldsymbol{e}}. \tag{8}$$

Using (5), one can write:

$$\begin{aligned}\dot{V}_R &= \dot{\boldsymbol{e}}^T(-\boldsymbol{K}_v\dot{\boldsymbol{e}} - \boldsymbol{K}_p\boldsymbol{e}) + \boldsymbol{e}^T\boldsymbol{K}_p\dot{\boldsymbol{e}} \\ &\quad - \dot{\boldsymbol{e}}^T\boldsymbol{C}_{eq}(\boldsymbol{x},\dot{\boldsymbol{x}})\dot{\boldsymbol{e}} + \frac{1}{2}\dot{\boldsymbol{e}}^T\dot{\boldsymbol{M}}_{eq}(\boldsymbol{x})\dot{\boldsymbol{e}} \\ &= -\dot{\boldsymbol{e}}^T\boldsymbol{K}_v\dot{\boldsymbol{e}} + \dot{\boldsymbol{e}}^T\left(\frac{1}{2}\dot{\boldsymbol{M}}_{eq}(\boldsymbol{x}) - \boldsymbol{C}_{eq}(\boldsymbol{x},\dot{\boldsymbol{x}})\right)\dot{\boldsymbol{e}}.\end{aligned}$$

According to property 2, the second term vanishes and therefore

$$\dot{V}_R = -\dot{\boldsymbol{e}}^T\boldsymbol{K}_v\dot{\boldsymbol{e}} \leq 0. \tag{9}$$

This implies that $\boldsymbol{e}$ and $\dot{\boldsymbol{e}}$ are bounded. Since the system (5) is nonautonomous, use Barbalat's lemma to complete the proof of asymptotic stability. In order to do that, let us check the uniform continuity of $\dot{V}_R$. The derivative of $\dot{V}_R$ is

$$\begin{aligned}\ddot{V}_R &= -2\dot{\boldsymbol{e}}^T\boldsymbol{K}_v\ddot{\boldsymbol{e}} \\ &= 2\dot{\boldsymbol{e}}^T\boldsymbol{K}_v\boldsymbol{M}_{eq}^{-1}(\boldsymbol{x})(\boldsymbol{C}_{eq}(\boldsymbol{x},\dot{\boldsymbol{x}})\dot{\boldsymbol{e}} + \boldsymbol{K}_p\boldsymbol{e} + \boldsymbol{K}_v\dot{\boldsymbol{e}}).\end{aligned}$$

This shows that $\ddot{V}_R$ is also bounded, since $\boldsymbol{e}$ and $\dot{\boldsymbol{e}}$ are bounded; hence, $\dot{V}_R$ is uniformly continuous. Applying Barbalat's lemma indicates that $\dot{\boldsymbol{e}} \to 0$ as $t \to \infty$. Hence, according to uniform continuity of $\ddot{\boldsymbol{e}}$, it can be concluded that $\ddot{\boldsymbol{e}} \to 0$ as $t \to \infty$. As a result, from (5), $\boldsymbol{K}_p\boldsymbol{e} \to \boldsymbol{0}$ as $t \to \infty$. Since $\boldsymbol{K}_p$ is a positive diagonal matrix, we may conclude that $\boldsymbol{x} \to \boldsymbol{x}_d$, as time tends to infinity and motion remains within the wrench–closure workspace.

III. Robot With Elastic Cables

A. Dynamic Model

As mentioned earlier, in a cable robot vibration caused by inevitable flexibility of cables shall be attenuated for applications that require high accuracy or high bandwidth. Thus, elasticity of cables is considered in this section. When elasticity in cables is considered in the modeling, actuator position is not directly related to the end–effector position. Hence, an augmented state vector may be considered, which consists of the position of actuators and the position of the end–effector. New research results have shown that in fully–constrained cable robots, dominant dynamics of cables are longitudinal vibrations [10] and therefore, axial spring model may suitably describe the effects of dominant dynamics of cable.

In order to model a general cable driven robot with n cables assume that: $L_{1i} : i = 1, 2, ..., n$ denotes the length of i^{th} cable with tension, which may be measured by a string pot or calculated by the solution of inverse kinematics problem. $L_{2i} : i = 1, 2, ..., n$ denotes the cable length of i^{th} actuator, which may be measured by the motor shaft encoder. If the system is rigid, then $L_{1i} = L_{2i}, \forall i$. Let us denote

$$\boldsymbol{L} = (L_{11}, L_{12}, \ldots, L_{1n}, L_{21}, L_{22}, \ldots, L_{2n})^T = (\boldsymbol{L}_1^T, \boldsymbol{L}_2^T)^T.$$

In a cable driven robot, the stiffness of cables is a function of cable lengths, which are changing during the motion of the robot. Furthermore, cables can be modeled by linear axial springs with Young's modulus E and cross-sectional area A. Therefore, the instantaneous potential energy of i^{th} cable is

$$p_i = \frac{EA(L_{1i} - L_{2i})^2}{2L_{2i}}. \tag{10}$$

The total potential energy of the system can be expressed by: $P = P_0 + P_1$, in which P_0 denotes the potential energy of the rigid robot and P_1 denotes the potential energy of the cables. Using linear axial spring model for cable and ignoring the effects of temperature, tension history etc., the total potential

energy of cables is given by

$$P_1 = \frac{1}{2}(\boldsymbol{L}_1 - \boldsymbol{L}_2)^T \boldsymbol{K}(\boldsymbol{L}_2)(\boldsymbol{L}_1 - \boldsymbol{L}_2) \tag{11}$$

where $\boldsymbol{K}$ is the stiffness matrix of the cables during the motion and is a function of $\boldsymbol{L}_2$. Suppose that all cables have the same Young's modulus E and cross-sectional area A, then

$$\boldsymbol{K}(\boldsymbol{L}_2) = EA \cdot \text{diag}^{-1}(\boldsymbol{L}_2). \tag{12}$$

Furthermore, kinetic energy of the system is

$$T = \frac{1}{2}\dot{\boldsymbol{x}}^T \boldsymbol{M}(\boldsymbol{x})\dot{\boldsymbol{x}} + \frac{1}{2}\dot{\boldsymbol{q}}^T \boldsymbol{I}_m \dot{\boldsymbol{q}}. \tag{13}$$

In which, $\boldsymbol{x}$ denotes the generalized coordinates in task space, $\boldsymbol{q}$ is the motor shaft position vector, $\boldsymbol{M}(\boldsymbol{x})$ is the mass matrix, and $\boldsymbol{I}_m$ is the actuator moments of inertia. Lagrangian function may be expressed as

$$\mathcal{L} = T - P = \frac{1}{2}\dot{\boldsymbol{x}}^T \boldsymbol{M}(\boldsymbol{x})\dot{\boldsymbol{x}} + \frac{1}{2}\dot{\boldsymbol{q}}^T \boldsymbol{I}_m \dot{\boldsymbol{q}} - P_0 - \frac{1}{2}(\boldsymbol{L}_1 - \boldsymbol{L}_2)^T \boldsymbol{K}(\boldsymbol{L}_2)(\boldsymbol{L}_1 - \boldsymbol{L}_2). \tag{14}$$

Using Euler–Lagrange formulation and some manipulations, final equations of motion can be written in the following form:

$$\boldsymbol{M}(\boldsymbol{x})\ddot{\boldsymbol{x}} + \boldsymbol{N}(\boldsymbol{x}, \dot{\boldsymbol{x}}) = \boldsymbol{J}^T \boldsymbol{K}(\boldsymbol{L}_2)(\boldsymbol{L}_2 - \boldsymbol{L}_1) \tag{15}$$

$$\boldsymbol{I}_m \ddot{\boldsymbol{q}} + r\boldsymbol{K}(\boldsymbol{L}_2)(\boldsymbol{L}_2 - \boldsymbol{L}_1) + r\boldsymbol{H}(\boldsymbol{L}_2, \boldsymbol{L}_1)(\boldsymbol{L}_2 - \boldsymbol{L}_1) = \boldsymbol{u} \tag{16}$$

in which,

$$\boldsymbol{N}(\boldsymbol{x}, \dot{\boldsymbol{x}}) = \boldsymbol{C}(\boldsymbol{x}, \dot{\boldsymbol{x}})\dot{\boldsymbol{x}} + \boldsymbol{G}(\boldsymbol{x}), \quad \boldsymbol{L}_2 - \boldsymbol{L}_0 = r\boldsymbol{q}$$

$$\boldsymbol{H}(\boldsymbol{L}_2, \boldsymbol{L}_1) = -\frac{1}{2}\boldsymbol{K}(\boldsymbol{L}_2)\,\text{diag}^{-1}(\boldsymbol{L}_2)\,\text{diag}(\boldsymbol{L}_2 - \boldsymbol{L}_1).$$

In these equations, $\boldsymbol{L}_0$ is the vector of cable length at $\boldsymbol{x} = 0$ and $\boldsymbol{J}$ is the Jacobian matrix of the system, which relates $\dot{\boldsymbol{x}}$ to the derivative of the cable length vector by $\dot{\boldsymbol{L}}_1 = \boldsymbol{J}\dot{\boldsymbol{x}}$, and other parameters are defined as before. Since in practice

$$\boldsymbol{I}_{n\times n} \gg -\frac{1}{2}\,\text{diag}^{-1}(\boldsymbol{L}_2)\,\text{diag}(\boldsymbol{L}_2 - \boldsymbol{L}_1) \tag{17}$$

where $\boldsymbol{I}_{n\times n}$ is $n \times n$ identity matrix. Thus, the equations of motion (15) and (16) can be written in the form of

$$\boldsymbol{M}(\boldsymbol{x})\ddot{\boldsymbol{x}} + \boldsymbol{N}(\boldsymbol{x}, \dot{\boldsymbol{x}}) = \boldsymbol{J}^T \boldsymbol{K}(\boldsymbol{L}_2 - \boldsymbol{L}_1) \tag{18}$$

$$\boldsymbol{I}_m \ddot{\boldsymbol{q}} + r\boldsymbol{K}(\boldsymbol{L}_2 - \boldsymbol{L}_1) = \boldsymbol{u}. \tag{19}$$

For notational simplicity, we assume that all cable stiffness constants are the same[1] and $\boldsymbol{K}$ is large with respect to other system parameters. To quantify how large the cable stiffness is with respect to other parameters, we assume that $\boldsymbol{K}$ is of the order $O(1/\epsilon^2)$ (ϵ is a small scalar parameter).

Equations (18) and (19) represent the cable driven robot as a nonlinear and coupled system. This representation includes both rigid and flexible subsystems and their interactions. It can be shown that the model of cable driven parallel robot with elastic cables may be reduced to (1), if the cable stiffness $\boldsymbol{K}$ tends to infinity. Furthermore, this model has inherited the properties of rigid dynamics (1), such as positive definiteness of inertia matrix and skew symmetricity of $\dot{\boldsymbol{M}} - 2\boldsymbol{C}$ [21].

[1]This assumption does not reduce the generality of problem. For general case, use variable scaling.

B. Control

In this section, we show that the control law (3) developed for a cable robot with nonelastic cables, can be modified for the robot with elastic cables. First, consider a composite control law by adding a corrective term to the control law (3) in the form of

$$\boldsymbol{u} = \boldsymbol{u}_r + \boldsymbol{K}_d(\dot{\boldsymbol{L}}_1 - \dot{\boldsymbol{L}}_2) \tag{20}$$

where $\boldsymbol{u}_r$ is given by (3) in terms of $\boldsymbol{x}$, and $\boldsymbol{K}_d$ is a constant positive diagonal matrix whose diagonal elements are in order of $O(1/\epsilon)$. Notice that

$$\boldsymbol{L}_2 = r\boldsymbol{q} + \boldsymbol{L}_0 \Longrightarrow \dot{\boldsymbol{L}}_2 = r\dot{\boldsymbol{q}} \quad \text{and} \quad \ddot{\boldsymbol{L}}_2 = r\ddot{\boldsymbol{q}}. \tag{21}$$

Substitute control law (20) in (19) and define variable $\boldsymbol{z}$ as

$$\boldsymbol{z} = \boldsymbol{K}(\boldsymbol{L}_2 - \boldsymbol{L}_1). \tag{22}$$

The closed loop dynamics reduces to:

$$r^{-1}\boldsymbol{I}_m \ddot{\boldsymbol{z}} + \boldsymbol{K}_d \dot{\boldsymbol{z}} + r\boldsymbol{K}\boldsymbol{z} = \boldsymbol{K}(\boldsymbol{u}_r - r^{-1}\boldsymbol{I}_m \ddot{\boldsymbol{L}}_1). \tag{23}$$

By the assumption on $\boldsymbol{K}$ and our choice for $\boldsymbol{K}_d$, we may assign

$$\boldsymbol{K} = \frac{\boldsymbol{K}_1}{\epsilon^2}; \quad \boldsymbol{K}_d = \frac{\boldsymbol{K}_2}{\epsilon} \tag{24}$$

where $\boldsymbol{K}_1$, $\boldsymbol{K}_2$ are of $O(1)$. Therefore, (23) can be written as

$$\epsilon^2 r^{-1}\boldsymbol{I}_m \ddot{\boldsymbol{z}} + \epsilon\boldsymbol{K}_2 \dot{\boldsymbol{z}} + r\boldsymbol{K}_1 \boldsymbol{z} = \boldsymbol{K}_1(\boldsymbol{u}_r - r^{-1}\boldsymbol{I}_m \ddot{\boldsymbol{L}}_1). \tag{25}$$

Now, (18) and (25) can be written together as

$$\boldsymbol{M}(\boldsymbol{x})\ddot{\boldsymbol{x}} + \boldsymbol{C}(\boldsymbol{x}, \dot{\boldsymbol{x}})\dot{\boldsymbol{x}} + \boldsymbol{G}(\boldsymbol{x}) = \boldsymbol{J}^T \boldsymbol{z} \tag{26}$$

$$\epsilon^2 r^{-1}\boldsymbol{I}_m \ddot{\boldsymbol{z}} + \epsilon\boldsymbol{K}_2 \dot{\boldsymbol{z}} + r\boldsymbol{K}_1 \boldsymbol{z} = \boldsymbol{K}_1(\boldsymbol{u}_r - r^{-1}\boldsymbol{I}_m \ddot{\boldsymbol{L}}_1). \tag{27}$$

The variable $\boldsymbol{z}$ and its time derivative $\dot{\boldsymbol{z}}$ may be considered the fast variables while the end–effector position variable $\boldsymbol{x}$ and its time derivative $\dot{\boldsymbol{x}}$ are considered the slow variables. Using the results of singular perturbation theory [22], elastic system (26) and (27) can be approximated by the quasi–steady state or slow subsystem and the boundary layer or fast subsystem as follows. With $\epsilon = 0$, (27) becomes

$$\bar{\boldsymbol{z}} = r^{-1}(\bar{\boldsymbol{u}}_r - r^{-1}\boldsymbol{I}_m \ddot{\bar{\boldsymbol{L}}}_1) \tag{28}$$

in which, the over bar variables represent the values of variables when $\epsilon = 0$. Substitute (28) into (26)

$$\boldsymbol{M}(\bar{\boldsymbol{x}})\ddot{\bar{\boldsymbol{x}}} + \boldsymbol{C}(\bar{\boldsymbol{x}}, \dot{\bar{\boldsymbol{x}}})\dot{\bar{\boldsymbol{x}}} + \boldsymbol{G}(\bar{\boldsymbol{x}}) = r^{-1}\boldsymbol{J}^T(\bar{\boldsymbol{u}}_r - r^{-1}\boldsymbol{I}_m \ddot{\bar{\boldsymbol{L}}}_1). \tag{29}$$

Furthermore, substitute $\ddot{\bar{\boldsymbol{L}}}_1 = \boldsymbol{J}\ddot{\bar{\boldsymbol{x}}} + \dot{\boldsymbol{J}}\dot{\bar{\boldsymbol{x}}}$ in the previous equation as

$$(r\boldsymbol{M}(\bar{\boldsymbol{x}}) + r^{-1}\boldsymbol{J}^T \boldsymbol{I}_m \boldsymbol{J})\ddot{\bar{\boldsymbol{x}}} + (r\boldsymbol{C}(\bar{\boldsymbol{x}}, \dot{\bar{\boldsymbol{x}}})\dot{\bar{\boldsymbol{x}}} + r^{-1}\boldsymbol{J}^T \boldsymbol{I}_m \dot{\boldsymbol{J}}\dot{\bar{\boldsymbol{x}}}) + r\boldsymbol{G}(\bar{\boldsymbol{x}}) = \boldsymbol{J}^T \bar{\boldsymbol{u}}_r \tag{30}$$

or equivalently

$$\boldsymbol{M}_{eq}(\bar{\boldsymbol{x}})\ddot{\bar{\boldsymbol{x}}} + \boldsymbol{C}_{eq}(\bar{\boldsymbol{x}}, \dot{\bar{\boldsymbol{x}}})\dot{\bar{\boldsymbol{x}}} + \boldsymbol{G}_{eq}(\bar{\boldsymbol{x}}) = \boldsymbol{J}^T \bar{\boldsymbol{u}}_r. \tag{31}$$

Equation (31) is called the quasi-steady state system. Notice that we were able to formulate (31) as the rigid model (1) in terms of slow variable $\bar{\boldsymbol{x}}$. Using Tikhonov's theorem [22], for $t > 0$, the elastic force $\boldsymbol{z}(t)$ and the end-effector position $\boldsymbol{x}(t)$ satisfy

$$\begin{aligned} \boldsymbol{z}(t) &= \bar{\boldsymbol{z}}(t) + \boldsymbol{\eta}(\tau) + O(\epsilon) \\ \boldsymbol{x}(t) &= \bar{\boldsymbol{x}}(t) + O(\epsilon) \end{aligned} \tag{32}$$

where, $\tau = t/\epsilon$ is the fast time scale and $\boldsymbol{\eta}$ is the fast state variable that satisfies the following boundary layer equation.

$$r^{-1}\boldsymbol{I}_m \frac{d^2\boldsymbol{\eta}}{d\tau^2} + \boldsymbol{K}_2 \frac{d\boldsymbol{\eta}}{d\tau} + r\boldsymbol{K}_1\boldsymbol{\eta} = \boldsymbol{0}. \tag{33}$$

Considering these results, elastic system (26) and (27) can be approximated up to $O(\epsilon)$ by

$$\boldsymbol{M}(\boldsymbol{x})\ddot{\boldsymbol{x}} + \boldsymbol{C}(\boldsymbol{x}, \dot{\boldsymbol{x}})\dot{\boldsymbol{x}} + \boldsymbol{G}(\boldsymbol{x}) = \boldsymbol{J}^T(\bar{\boldsymbol{z}} + \boldsymbol{\eta}(\tau)) \tag{34}$$

$$r^{-1}\boldsymbol{I}_m \frac{d^2\boldsymbol{\eta}}{d\tau^2} + \boldsymbol{K}_2 \frac{d\boldsymbol{\eta}}{d\tau} + r\boldsymbol{K}_1\boldsymbol{\eta} = \boldsymbol{0}. \tag{35}$$

According to (28)

$$\boldsymbol{M}_{eq}(\boldsymbol{x})\ddot{\boldsymbol{x}} + \boldsymbol{C}_{eq}(\boldsymbol{x}, \dot{\boldsymbol{x}})\dot{\boldsymbol{x}} + \boldsymbol{G}_{eq}(\boldsymbol{x}) = \boldsymbol{J}^T(\boldsymbol{u}_r + r\boldsymbol{\eta}(\tau)) \tag{36}$$

$$r^{-1}\boldsymbol{I}_m \frac{d^2\boldsymbol{\eta}}{d\tau^2} + \boldsymbol{K}_2 \frac{d\boldsymbol{\eta}}{d\tau} + r\boldsymbol{K}_1\boldsymbol{\eta} = \boldsymbol{0}. \tag{37}$$

Notice that the controller gain $\boldsymbol{K}_2$ can be suitably chosen such that the boundary layer system (37) becomes asymptotically stable. By this means, with sufficiently small values of ϵ, the response of the elastic system (18) and (19) with the composite control (20) consisting of the rigid control $\boldsymbol{u}_r$ given by (3) and the corrective term $\boldsymbol{K}_d(\dot{\boldsymbol{L}}_1 - \dot{\boldsymbol{L}}_2)$, will be nearly the same as the response of rigid system (1) with the rigid control $\boldsymbol{u}_r$ alone. This happens after some initially damped transient oscillation of fast variables $\boldsymbol{\eta}(t/\epsilon)$.

C. Stability Analysis of the Total System

Control of the rigid model and its stability analysis were discussed in previous section. It is demonstrated that the boundary layer or the fast subsystem (33) is asymptotically stable, if the corrective term is used in the control law. However, in general, individual stability of boundary layer and that of quasi-steady state subsystems does not guarantee the stability of total closed-loop system. In this section, the stability of the total system is analyzed in detail. Recall the dynamic equations of elastic system (36) and (37), and apply the control law (3) from previous section. This results in

$$\boldsymbol{M}_{eq}(\boldsymbol{x})\ddot{\boldsymbol{e}} + (\boldsymbol{C}_{eq}(\boldsymbol{x}, \dot{\boldsymbol{x}}) + \boldsymbol{K}_v)\dot{\boldsymbol{e}} + \boldsymbol{K}_p\boldsymbol{e} = -r\boldsymbol{J}^T\boldsymbol{\eta}(t/\epsilon) \tag{38}$$

$$r^{-1}\boldsymbol{I}_m \frac{d^2\boldsymbol{\eta}}{dt^2} + \boldsymbol{K}_d \frac{d\boldsymbol{\eta}}{dt} + r\boldsymbol{K}\boldsymbol{\eta} = \boldsymbol{0}. \tag{39}$$

Consider $\boldsymbol{y} = \begin{bmatrix} \boldsymbol{e} \\ \dot{\boldsymbol{e}} \end{bmatrix}$ and $\boldsymbol{h} = \begin{bmatrix} \boldsymbol{\eta} \\ \dot{\boldsymbol{\eta}} \end{bmatrix}$, in which, $\boldsymbol{e} = \boldsymbol{x}_d - \boldsymbol{x}$, then

$$\dot{\boldsymbol{y}} = \boldsymbol{A}\boldsymbol{y} + \boldsymbol{B}\begin{bmatrix} \boldsymbol{I} & \boldsymbol{0} \end{bmatrix}\boldsymbol{h} \tag{40}$$

$$\dot{\boldsymbol{h}} = \tilde{\boldsymbol{A}}\boldsymbol{h} \tag{41}$$

in which

$$\boldsymbol{A} = \begin{bmatrix} \boldsymbol{0} & \boldsymbol{I} \\ -\boldsymbol{M}_{eq}^{-1}\boldsymbol{K}_p & -\boldsymbol{M}_{eq}^{-1}(\boldsymbol{K}_v + \boldsymbol{C}_{eq}) \end{bmatrix}$$

$$\boldsymbol{B} = \begin{bmatrix} \boldsymbol{0} \\ -r\boldsymbol{M}_{eq}^{-1}\boldsymbol{J}^T \end{bmatrix}$$

$$\tilde{\boldsymbol{A}} = \begin{bmatrix} \boldsymbol{0} & \boldsymbol{I} \\ -r^2\boldsymbol{I}_m^{-1}\boldsymbol{K} & -r\boldsymbol{I}_m^{-1}\boldsymbol{K}_d \end{bmatrix}.$$

Then, the stability of this system may be analyzed by the following lemma.

Lemma 1: There is a positive definite matrix $\boldsymbol{K}_d$ such that the closed-loop system described by the state space representation (41), is asymptotically stable.

Proof: Consider the following Lyapunov function candidate:

$$V_F = \boldsymbol{h}^T\boldsymbol{W}\boldsymbol{h}, \quad \boldsymbol{W} = \frac{1}{2}\begin{bmatrix} r^2(\boldsymbol{K}_d + \boldsymbol{K}) & r\boldsymbol{I}_m \\ r\boldsymbol{I}_m & \boldsymbol{I}_m \end{bmatrix}. \tag{42}$$

According to Schur complement, in order to have positive definite $\boldsymbol{W}$, it is sufficient to have $\boldsymbol{K}_d > \boldsymbol{I}_m$. Differentiate V_F along trajectories of (41)

$$\begin{aligned} \dot{V}_F &= \dot{\boldsymbol{h}}^T\boldsymbol{W}\boldsymbol{h} + \boldsymbol{h}^T\boldsymbol{W}\dot{\boldsymbol{h}} + \boldsymbol{h}^T\dot{\boldsymbol{W}}\boldsymbol{h} \\ &= -r^3\boldsymbol{\eta}^T\boldsymbol{K}\boldsymbol{\eta} - r\dot{\boldsymbol{\eta}}^T(\boldsymbol{K}_d - \boldsymbol{I}_m)\dot{\boldsymbol{\eta}}. \end{aligned} \tag{43}$$

$\dot{V}_F$ can be written as

$$\dot{V}_F = -\boldsymbol{h}^T\boldsymbol{S}\boldsymbol{h}, \quad \boldsymbol{S} = \begin{bmatrix} r^3\boldsymbol{K} & \boldsymbol{0} \\ \boldsymbol{0} & r(\boldsymbol{K}_d - \boldsymbol{I}_m) \end{bmatrix}. \tag{44}$$

Since, $\boldsymbol{K}, \boldsymbol{K}_d$, and $\boldsymbol{I}_m$ are diagonal positive definite matrices, $\dot{V}_F$ becomes negative definite if $\boldsymbol{K}_d > \boldsymbol{I}_m$. If this condition holds, the closed-loop system (41) is asymptotically stable. ■

Theorem 1: The closed-loop system (40) and (41) is asymptotically stable, by proper selection of controller gains $\boldsymbol{K}_v$, and $\boldsymbol{K}_d$.

Proof: Consider the following composite Lyapunov function candidate

$$V(\boldsymbol{y}, \boldsymbol{h}) = V_R + V_F \tag{45}$$

in which, V_R denotes the Lyapunov function candidate for the rigid subsystem given in (7), and V_F denotes that for the fast subsystem (33), given in (42). Differentiate $V(\boldsymbol{y}, \boldsymbol{h})$ along trajectories of (40) and (41). Hence

$$\dot{V}(\boldsymbol{y}, \boldsymbol{h}) = \dot{V}_R + \dot{V}_F = -\dot{\boldsymbol{e}}^T\boldsymbol{K}_v\dot{\boldsymbol{e}} - r\dot{\boldsymbol{e}}^T\boldsymbol{J}^T\boldsymbol{\eta} - \boldsymbol{h}^T\boldsymbol{S}\boldsymbol{h}. \tag{46}$$

According to Rayleigh–Ritz inequality

$$-\boldsymbol{h}^T\boldsymbol{S}\boldsymbol{h} \leq -\lambda_{\min}(\boldsymbol{S})\|\boldsymbol{h}\|^2. \tag{47}$$

Therefore

$$-\dot{\boldsymbol{e}}^T\boldsymbol{K}_v\dot{\boldsymbol{e}} \leq -\lambda_{\min}(\boldsymbol{K}_v)\|\dot{\boldsymbol{e}}\|^2 \tag{48}$$

$$-r\dot{\boldsymbol{e}}^T\boldsymbol{J}^T\boldsymbol{\eta} \leq r\sigma_{\max}(\boldsymbol{J}^T)\|\dot{\boldsymbol{e}}\|\|\boldsymbol{h}\| \tag{49}$$

in which $\lambda_{\min}$ and $\sigma_{\max}$ denote the smallest eigenvalue and largest singular value of the corresponding matrices, respectively. Using the above inequalities, one may write

$$\begin{aligned} &\dot{V}(\boldsymbol{y}, \boldsymbol{h}) \leq \\ &-\lambda_{\min}(\boldsymbol{K}_v)\|\dot{\boldsymbol{e}}\|^2 + r\sigma_{\max}(\boldsymbol{J}^T)\|\dot{\boldsymbol{e}}\|\|\boldsymbol{h}\| - \lambda_{\min}(\boldsymbol{S})\|\boldsymbol{h}\|^2 \end{aligned}$$

or equivalently

$$\dot{V}(\boldsymbol{y},\boldsymbol{h}) \leq \begin{bmatrix}\|\dot{\boldsymbol{e}}\| & \|\boldsymbol{h}\|\end{bmatrix}\begin{bmatrix}-\lambda_{\min}(\boldsymbol{K}_v) & 0.5r\sigma_{\max}(\boldsymbol{J}^T)\\ 0.5r\sigma_{\max}(\boldsymbol{J}^T) & -\lambda_{\min}(\boldsymbol{S})\end{bmatrix}\begin{bmatrix}\|\dot{\boldsymbol{e}}\|\\ \|\boldsymbol{h}\|\end{bmatrix}.$$

In order to have $\dot{V}(\boldsymbol{y},\boldsymbol{h}) \leq 0$, it is sufficient to satisfy the following inequality:

$$\lambda_{\min}(\boldsymbol{K}_v)\lambda_{\min}(\boldsymbol{S}) > 0.25\, r^2\sigma^2_{\max}(\boldsymbol{J}^T). \tag{50}$$

This condition is simply met by choosing appropriate values for $\boldsymbol{K}_v$ in (3) and $\boldsymbol{K}_d$ for fast subsystem. Enforcing $\dot{V}(\boldsymbol{y},\boldsymbol{h})$ to be negative semidefinite, implies that $\boldsymbol{y}$ and $\boldsymbol{h}$ are bounded. This indicates that $\ddot{V}(\boldsymbol{y},\boldsymbol{h})$ is bounded. Hence, $\dot{V}(\boldsymbol{y},\boldsymbol{h})$ is uniformly continuous. Like before, by using Barbalat's lemma, one may conclude that $\dot{\boldsymbol{e}} \to 0$ and $\boldsymbol{h} \to 0$ as $t \to \infty$. According to uniform continuity of $\ddot{\boldsymbol{e}}$, it can be concluded that $\ddot{\boldsymbol{e}} \to 0$ as $t \to \infty$. As a result, the total closed-loop system (40) and (41) becomes asymptotically stable. ■

The control gains $\boldsymbol{K}_p$ and $\boldsymbol{K}_v$ are obtained according to asymptotic stability of the corresponding rigid model (31). In addition, $\boldsymbol{K}_v$ and $\boldsymbol{K}_d$ should be chosen so as they satisfy equation (50) and negative definiteness of $\boldsymbol{S}$. Furthermore, $\boldsymbol{K}_d$ determines damping rate of the vibrations caused by fast variables $\boldsymbol{\eta}(t)$.

Remark 1: In design procedure of the controller, it is assumed that the Jacobian matrix of the cable robot is nonsingular and at all times, positive internal forces can be generated such that the cables remain in tension.

Remark 2: Internal forces can change the cables tensions. As a consequence, the elastic forces $-\boldsymbol{z} = \boldsymbol{K}(\boldsymbol{L}_1 - \boldsymbol{L}_2)$ and fast variable $\boldsymbol{\eta}(t)$ will be affected and this can cause vibrations in the mechanism. However, as proved in lemma 1, because of using corrective term $\boldsymbol{K}_d(\dot{\boldsymbol{L}}_1 - \dot{\boldsymbol{L}}_2)$ in the proposed control algorithm (20), the fast or boundary subsystem (39) is asymptotically stable and thus, the resulting vibrations are efficiently damped.

Remark 3: In a cable robot with high elasticity in cables, according to remark 1, choosing high gains for $\boldsymbol{K}_v$ may limit the reachable workspace. In this case, the choice of $\boldsymbol{K}_v$ is related to the volume of the desired reachable workspace. This subject is under current research.

IV. Case Study

In order to verify the effectiveness of the proposed control algorithm, a simulation study has been performed on a spatial cable driven manipulator. KNTU cable robot is a fully–constrained spatial cable manipulator actuated by eight cables. This manipulator is under investigation for possible high speed and wide workspace applications at K. N. Toosi University [30]. There exist different designs for KNTU cable robot based on different approaches such as collision avoidance scheme, force feasibility, and dexterity. A special design of KNTU cable robot is shown in Fig. 1, which is called Galaxy. This manipulator possesses six degrees of freedom with two degrees of actuator redundancy.

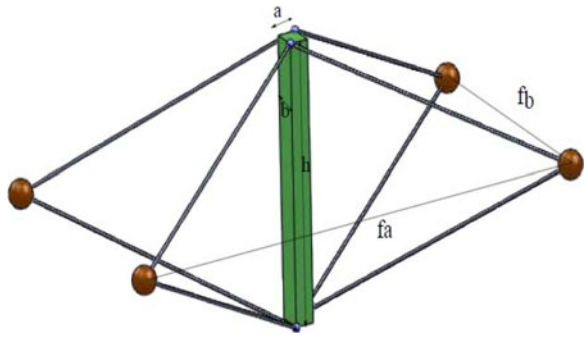

Fig. 1. Schematics of KNTU Galaxy design [30].

Consider $\boldsymbol{x} = [x_p, y_p, z_p, \alpha, \beta, \gamma]^T$ as generalized coordinates vector, in which $\boldsymbol{\theta} = [\alpha, \beta, \gamma]^T$ denotes the vector of a set of Pitch–Roll–Yaw Euler angles. With this definition, the angular velocity of the end-effector can be written in the following form:

$$\boldsymbol{\omega} = \boldsymbol{E}\dot{\boldsymbol{\theta}}, \quad \dot{\boldsymbol{\theta}} = \left[\dot{\alpha}, \dot{\beta}, \dot{\gamma}\right]^T \tag{51}$$

in which

$$\boldsymbol{E} = \begin{bmatrix}\cos(\beta)\cos(\gamma) & -\sin(\gamma) & 0\\ \cos(\beta)\sin(\gamma) & \cos(\gamma) & 0\\ -\sin(\beta) & 0 & 1\end{bmatrix}.$$

With this notation, the equations of motion can be written in terms of $\boldsymbol{x}$. By some manipulations, these equations may be derived as [26]

$$\boldsymbol{M}(\boldsymbol{x})\ddot{\boldsymbol{x}} + \boldsymbol{C}(\boldsymbol{x},\dot{\boldsymbol{x}})\dot{\boldsymbol{x}} + \boldsymbol{G}(\boldsymbol{x}) = \boldsymbol{F} \tag{52}$$

where

$$\boldsymbol{M}(\boldsymbol{x}) = \begin{bmatrix}m\boldsymbol{I}_{3\times3} & \boldsymbol{0}_{3\times3}\\ \boldsymbol{0}_{3\times3} & \boldsymbol{E}^T\boldsymbol{I}_P\boldsymbol{E}\end{bmatrix} \tag{53}$$

$$\boldsymbol{C}(\boldsymbol{x},\dot{\boldsymbol{x}})\dot{\boldsymbol{x}} = \begin{bmatrix}\boldsymbol{0}_{3\times1}\\ \boldsymbol{E}^T\{\boldsymbol{I}_P\dot{\boldsymbol{E}}\dot{\boldsymbol{\theta}} + (\boldsymbol{E}\dot{\boldsymbol{\theta}})\times\boldsymbol{I}_P(\boldsymbol{E}\dot{\boldsymbol{\theta}})\}\end{bmatrix} \tag{54}$$

$$\boldsymbol{G}(\boldsymbol{x}) = \begin{bmatrix}-m\boldsymbol{g}\\ \boldsymbol{0}_{3\times1}\end{bmatrix}. \tag{55}$$

In these equations, m denotes the mass of the end-effector; $\boldsymbol{I}_P$ denotes the inertia tensor of the end-effector; $\boldsymbol{I}_{3\times3}$ is a 3×3 identity matrix, and $\boldsymbol{g}$ denotes the gravity acceleration vector. By considering elasticity in the cables, the system components are given as follows:

$$\boldsymbol{F} = \boldsymbol{J}^T\boldsymbol{K}(\boldsymbol{L}_2 - \boldsymbol{L}_1),\ \boldsymbol{L}_2 = r\boldsymbol{q} + \boldsymbol{L}_0$$
$$\boldsymbol{I}_m\ddot{\boldsymbol{q}} + r\boldsymbol{K}(\boldsymbol{L}_2 - \boldsymbol{L}_1) = \boldsymbol{u}. \tag{56}$$

The following parametric values in SI units are used in the simulations; $\boldsymbol{I}_m = 0.6\,\boldsymbol{I}_{8\times8}$, $r = 0.035$, $\boldsymbol{K} = 1000\,\boldsymbol{I}_{8\times8}$, $m = 2.5$, and $I_P = \mathrm{diag}[0.212, 0.225, 0.03]$. In order to demonstrate a high flexible system, $\boldsymbol{K}$ is intentionally set very low. To show the effectiveness of the proposed composite control algorithm, suppose that the system is at the origin and has to track the following smooth reference trajectories in task

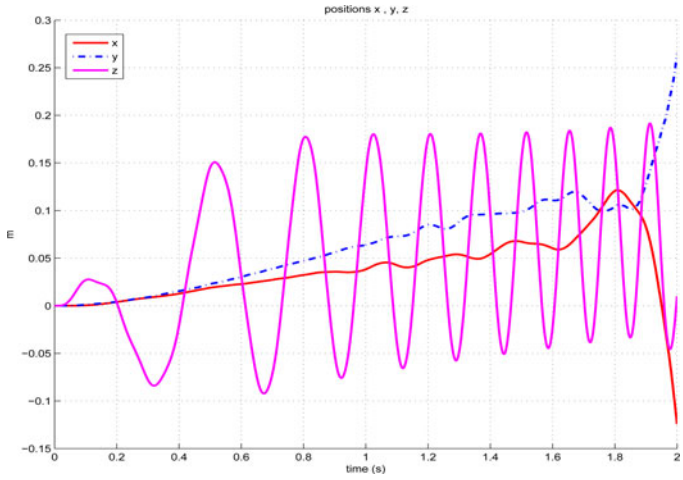

Fig. 2. Closed-loop system experiences instability, if only rigid controller $\boldsymbol{u}_r$ is applied.

space coordinates

$$x_d = y_d = 0.3 + 1.5e^{-t} - 1.8e^{-t/1.2}$$
$$z_d = 0.2 + e^{-t} - 1.2e^{-t/1.2}$$
$$\alpha_d = \beta_d = 0$$
$$\gamma_d = 0.2 + e^{-t} - 1.2e^{-t/1.2}$$

in which, the translational task space variables x_P, y_P, and z_P, and rotational task space variables α_P, β_P, and γ_P reach a final value of 0.3 m, 0.3 m, 0.2 m, 0 rad, and 0.2 rad from the zero states, respectively. The controller is based on (20) and consists of rigid control $\boldsymbol{u}_r$ given by (3) and the corrective term. Controller gain matrices are chosen as $\boldsymbol{K}_p = 250\ \boldsymbol{I}_{6\times 6}, \boldsymbol{K}_v = 30\ \boldsymbol{I}_{6\times 6}$, and $\boldsymbol{K}_d = 550\ \boldsymbol{I}_{8\times 8}$ to satisfy the stability conditions. In the first step, rigid control $\boldsymbol{u}_r$ alone is applied to the manipulator. As illustrated in Fig. 2, the manipulator experiences instability if only the rigid control $\boldsymbol{u}_r$ is applied to the system. The main reason for instability is the divergence of its fast variables.

Fig. 3 illustrates dynamic behavior of the closed-loop system with the proposed control algorithm. Internal force $\boldsymbol{Q}$ is used whenever at least one cable becomes slack (or $L_{1i} < L_{2i}$, $i = 1, \ldots, 8$) to ensure that the cables remain in tension. Although the system is very flexible, the proposed control algorithm can suitably stabilize the system. As seen in this figure, position and orientation outputs track the desired values very well and the steady state errors are very small, while as it is shown in Fig. 4, all cables are in tension for the whole maneuver.

To compare the performance of the proposed control algorithm with respect to the traditional (rigid) one, a more realistic case study with $\boldsymbol{K} = 10000\ \boldsymbol{I}_{8\times 8}$ is considered. In this simulation, suppose that the home position for the end-effector is zero and the desired end-effector position and orientation are

$$x_d = 0.2(1 - e^{-t})$$
$$y_d = z_d = 0$$
$$\alpha_d = \beta_d = \gamma_d = 0.$$

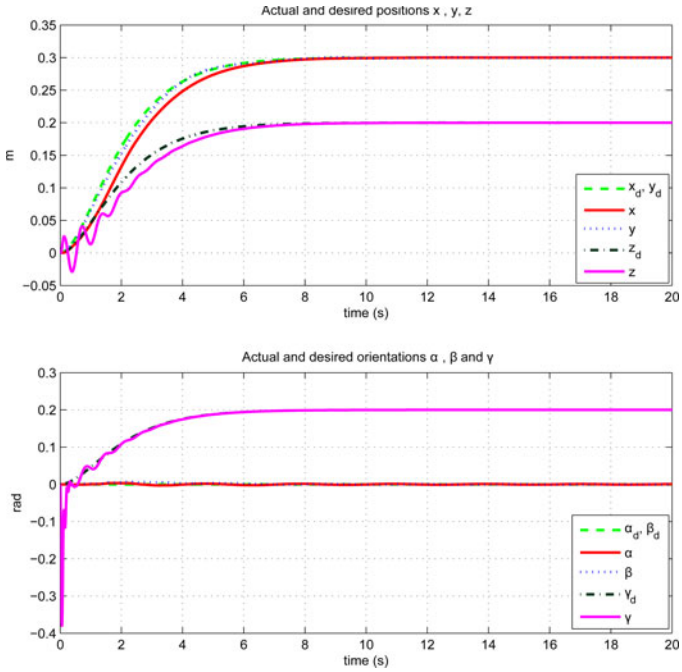

Fig. 3. Suitable tracking performance of the closed-loop system to smooth reference trajectories; proposed control algorithm.

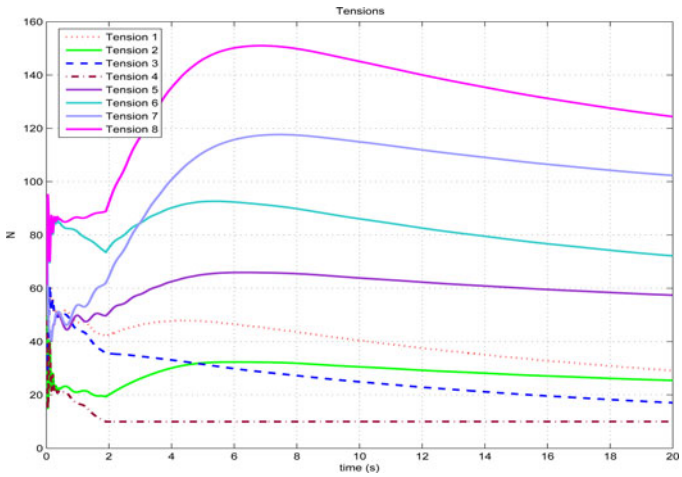

Fig. 4. Simulation results showing the cables tension for smooth reference trajectories.

As illustrated in Fig. 5, the closed-loop system becomes stable however there exists vibrations in the output, provided that only the corresponding rigid control effort $\boldsymbol{u}_r$ is applied on the system. These vibrations limit the absolute accuracy and bandwidth of the mechanism which are very important in many applications such as high speed manipulation. However, as illustrated in Fig. 6, the system becomes stable and the desired trajectories are well tracked by using the proposed control algorithm. Moreover, as it is shown in Fig. 7, all cable tensions are positive.

To investigate the effects of internal forces on the performances of the closed–loop system, another simulation is performed. In this simulation, the following reference trajectories are chosen such that the end-effector approaches near the

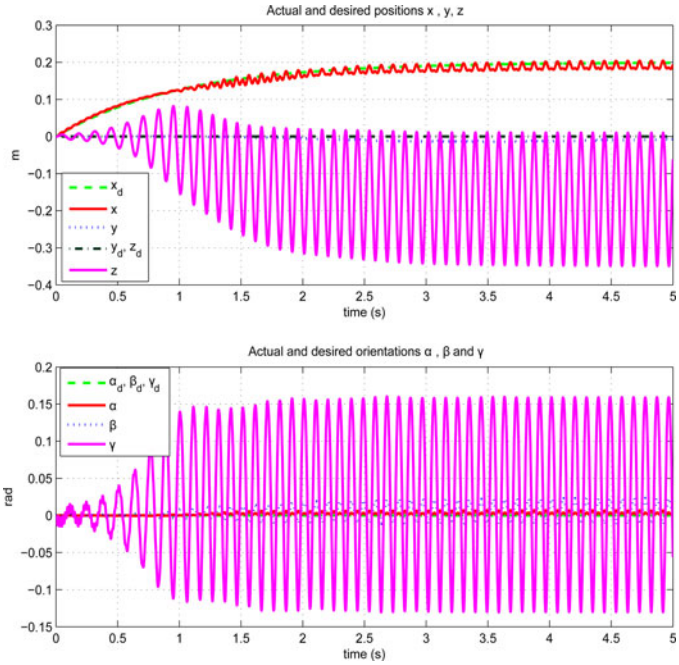

Fig. 5. Tracking performance of the closed-loop system with $\boldsymbol{K} = 10^4 \boldsymbol{I}_{8\times 8}$, if only rigid controller $\boldsymbol{u}_r$ is applied.

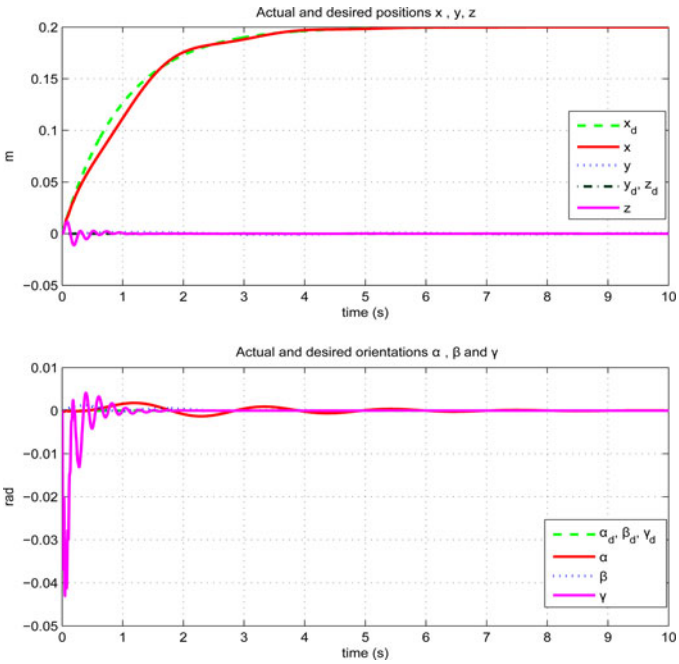

Fig. 6. Suitable tracking performance of the closed-loop system with $\boldsymbol{K} = 10^4 \boldsymbol{I}_{8\times 8}$; proposed control algorithm.

boundary of the wrench-closure workspace

$$x_d = y_d = 0$$
$$z_d = 0.42 - 0.42e^{-2t}$$
$$\alpha_d = \beta_d = \gamma_d = 0.$$

In this trajectory, the task space variable z_P reaches the final value of 0.42 m, which is near the boundary of the workspace.

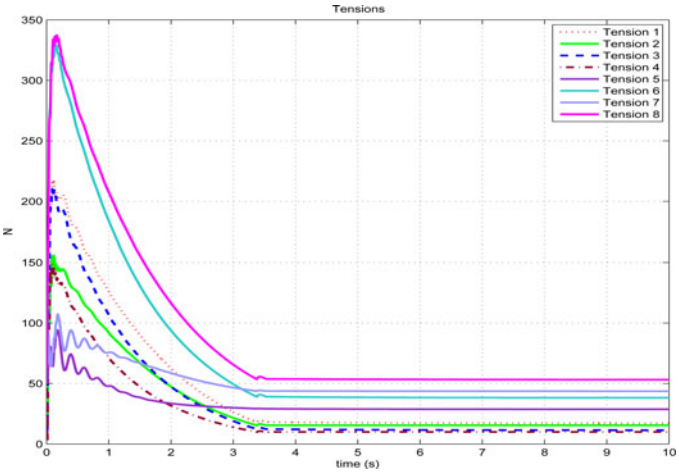

Fig. 7. Simulation results showing the cables tension with $\boldsymbol{K} = 10^4 \boldsymbol{I}_{8\times 8}$; proposed control algorithm.

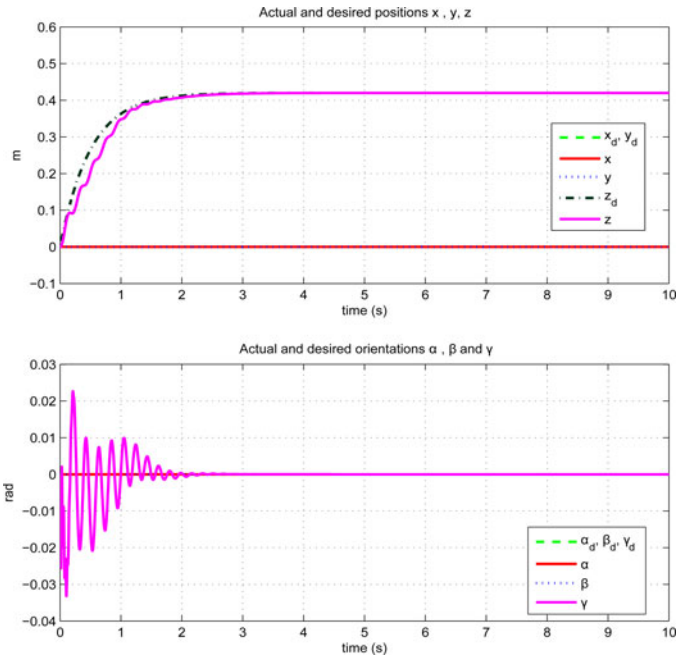

Fig. 8. Tracking performance of the closed-loop system when the end–effector approaches near the boundary of the workspace.

A well known result in the literature on cable robots reports that a pose is fully-constrained if and only if the corresponding wrench matrix $\boldsymbol{W}_r$ (in this paper, $-\boldsymbol{J}$) is of full rank and there exists a positive vector $\boldsymbol{t} > 0$ in the null space of $\boldsymbol{W}_r$ [8]. According to this result, near the boundaries of the wrench-closure workspace, some elements of the vector $\boldsymbol{t}$ are near zero and thus internal forces, which are used to avoid cable slackening, may become very high for a number of cables. Simulation results confirm this fact, as shown in Figs. 8 and 9, the internal forces in cable 7 and 8 are high in this case.

The internal forces among the cables are increased in the next simulation by setting the minimum tension force to 100. As illustrated in Fig. 10, and notice the scale of figures of Euler angles, it is observed that the deviations from zero desired

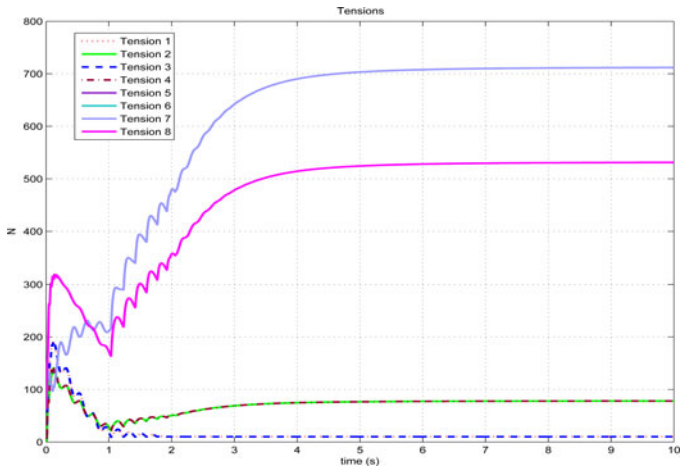

Fig. 9. Cables tension when the end–effector approaches near the boundary of the workspace.

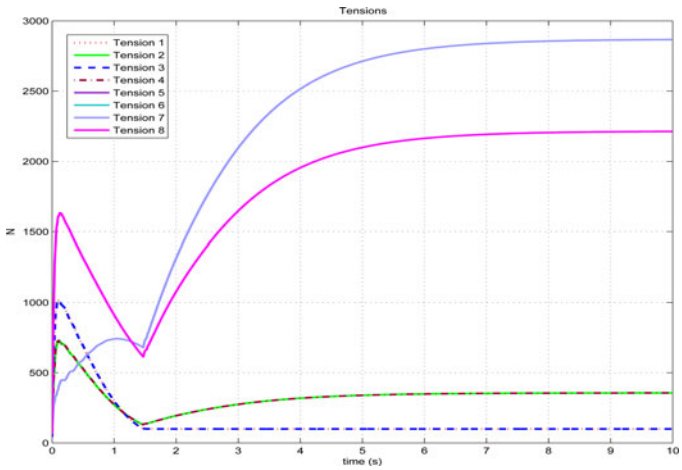

Fig. 11. Cables tension when the end–effector approaches near the boundary of the workspace and the internal forces increase.

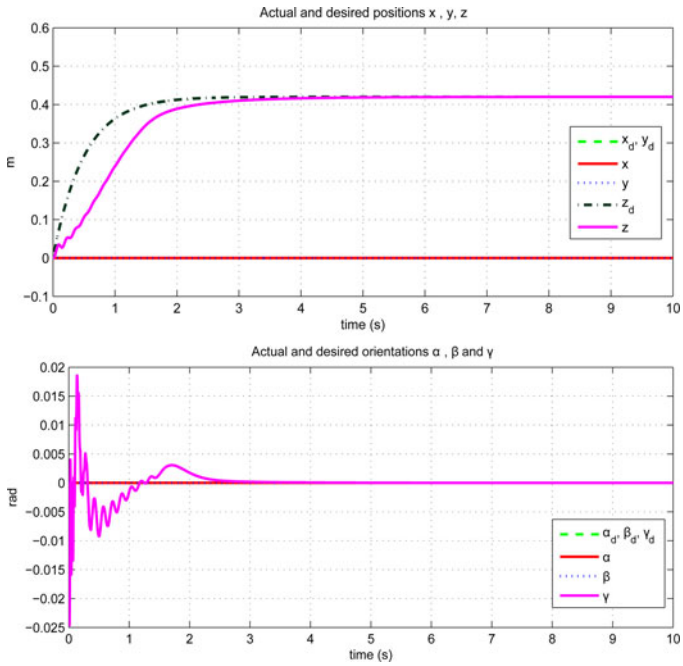

Fig. 10. Tracking performance of the closed-loop system when the end–effector approaches near the boundary of the workspace and the internal forces increase.

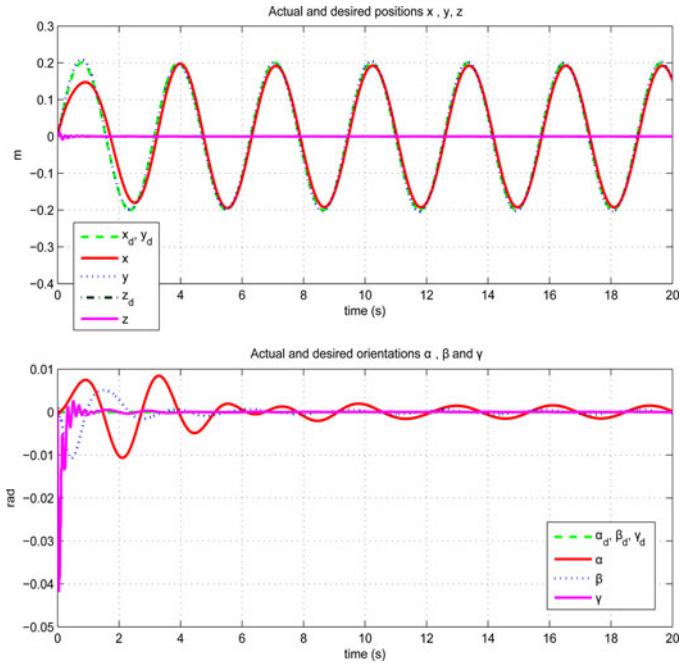

Fig. 12. Suitable tracking performance of the closed-loop system to sinusoid reference trajectories; proposed control algorithm.

value in these variables are lower than that shown in Fig. 8. This confirms that since the pose is stabilizable the equivalent stiffness has increased. However, as shown in Fig. 10, the error in z direction is larger than that shown in Fig. 8, and furthermore, the response is slower than when the minimum tensions is set to 10. This observation confirms that by increasing the internal forces, the elastic forces and the overall stiffness of the manipulator are increased. Therefore, the amplitude of high oscillation may decrease while the frequency of them may increase. However, the proposed control law is still capable to damp the oscillation of fast variable and stabilize the total motion of the robot, although the transient of the motion will be changed.

In order to verify the reachable bandwidth of the closed-loop system, another simulation is performed. The following reference trajectories are considered for this simulation:

$$x_d = y_d = 0.2\sin(2t)$$

while the other parameters are set to zero. Fig. 12 shows the reference and actual trajectories of x, y, and deviation of the other parameters from its zero desired value. It can be seen that the proposed control scheme is capable of performing such a maneuver, while the positioning errors remain small. Furthermore, as shown in Fig. 13, it is observed that all tensions in the cables for this test remain positive as well. The simulation results illustrate the guaranteed stability of the system with the proposed controller for the manipulator with elastic cables.

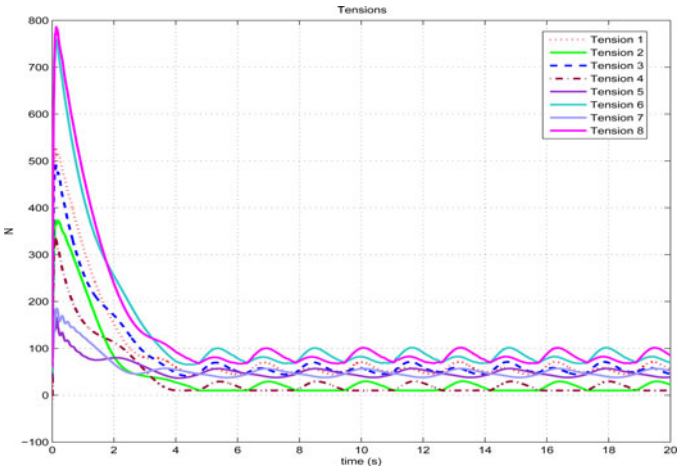

Fig. 13. Simulation results showing the cables tension for sinusoid reference trajectories.

V. Conclusion

This paper addresses stability analysis and control of fully-constrained cable driven robots with elastic cables. Inevitable elasticity of cables has negative impacts on accuracy and bandwidth of the cable robot. Thus, to cope with vibrations caused by cable elasticity, control scheme shall be designed to minimize the effects of elasticity on the closed–loop performance. In order to accomplish this goal, with assumption of axial spring model for the cable, dynamics of fully–constrained cable robot is derived and a composite control algorithm is proposed to achieve suitable tracking performance. This controller consists of two major parts: 1) a rigid controller, which is based on a rigid model of the system; and 2) a corrective term added for vibrational damping. Then, the closed loop dynamic equations of motion are converted to the standard form of singular perturbation formulation. This representation allows the use of singular perturbation theory in the course of controller design. Based on these results, two subsystems, namely slow and fast, are separated and incorporated in to the stability analysis of the total closed-loop system. Stability of the total closed-loop system is analyzed through the Lyapunov second method and the stability conditions are derived for the closed-loop system. Finally, the performance of the proposed controller is examined through simulation studies on a spatial cable robot.

References

[1] H. D. Taghirad and M. Nahon, "Kinematic analysis of a macro–micro redundantly actuated parallel manipulator," *Adv. Robot.*, vol. 22, no. 6–7, pp. 657–687, 2008.

[2] S. Kawamura, H. Kino, and C. Won, "High-speed manipulation by using parallel wire-driven robots," *Robotica*, vol. 18, no. 3, pp. 13–21, 2000.

[3] R. Bostelman, J. Albus, N. Dagalakis, and A. Jacoff, "Applications of the NIST robocrane," in *Proc. 5th Int. Symp. Robot. Manuf.*, 1994, pp. 403–410.

[4] R. Roberts, T. Graham, and T. Lippitt, "On the inverse kinematics, statics, and fault tolerance of cable-suspended robots," *J. Robot. Syst.*, vol. 15, no. 10, pp. 649–661, 1998.

[5] A. Riechel, P. Bosscher, H. Lipkin, and I. Ebert-Uphoff, "Concept paper: Cable-driven robots for use in hazardous environments," in *Proc. 10th Int. Top. Meet. Robot Remote Syst. Hazard. Environ.*, Gainesville, FL, USA, 2004, pp. 310–317.

[6] P. M. Bosscher, "Disturbance robustness measures and wrench-feasible workspace generation techniques for cable-driven manipulators" Ph.D. dissertation, George W. Woodruff Sch. Mech. Eng., Georgia Inst. Technol., Atlanta, GA, USA, 2004, 197 pp..

[7] W. B Lim, G. Yang, S. H Yeo, and S. K. Mustafa, "A generic force-closure analysis algorithm for cable-driven parallel manipulators," *Mech. Mach. Theory*, vol. 46, no. 9, pp. 1265–1275, 2011.

[8] M. Gouttefarde, "Characterizations of fully-constrained poses of parallel cable-driven robots: A review," in *Proc. ASME Int. Design Eng. Tech. Conf.*, 2008, pp. 3–6.

[9] P. M. Bosscher, A. T. Riechel, and I. Ebert-Uphoff, "Wrench-feasible workspace generation for cable-driven robots," *IEEE Trans. Robot.*, vol. 22, no. 5, pp. 890–902, Oct. 2006.

[10] X. Diao and O. Ma, "Vibration analysis of cable-driven parallel manipulators," *Multibody Syst. Dyn.*, vol. 21, pp. 347–360, 2009.

[11] A. Alp and S. Agrawal, "Cable suspended robots: Feedback controllers with positive inputs," in *Proc. Amer. Control Conf.*, 2002, pp. 815–820.

[12] R. L. Williams, P. Gallina, and J. Vadia, "Planar translational cable direct driven robots," *J. Robot. Syst.*, vol. 20, no. 3, pp. 107–120, 2003.

[13] S. Ryoek and S. Agrawal, "Generation of feasible set points and control of a cable robot," *IEEE Trans. Robot.*, vol. 22, no. 3, pp. 551–558, Jun. 2006.

[14] M. A. Khosravi and H. D. Taghirad. (2013). "Robust PID control of fully-constrained cable drive parallel robots," *Mechatronics*, [Online]. Available:http://dx.doi.org/10.1016/j.mechatronics.2013.12.001

[15] H. Kino, T. Yahiro, and F. Takemura, "Robust PD control using adaptive compensation for completely restrained parallel-wire driven robots," *IEEE Trans. Robot.*, vol. 23, no. 4, pp. 803–812, Aug. 2007.

[16] S. Fang, D. Franitza, M. Torlo, F. Bekes, and M. Hiller, "Motion control of a tendon-based parallel manipulator using optimal tension distribution," *IEEE/ASME Trans. Mechatronics*, vol. 9, no. 3, pp. 561–568, Sep. 2004.

[17] Q. Jiang and V. Kumar, "The inverse kinematics of cooperative transport with multiple aerial robots," *IEEE Trans. Robot.*, vol. 29, no. 1, pp. 136–145, Feb. 2013.

[18] J. Gorman, K. Jablokow, and D. Cannon, "The cable array robot: Theory and experiment," in *Proc. IEEE Int. Conf. Robot. Autom.*, 2001, pp. 2804–2810.

[19] E. Ottaviano and G. Castelli, "A study on the effects of cable mass and elasticity in cable-based parallel manipulators," *ROMANSY 18 Robot Design, Dyn. Control*, vol. 524, ch. I, pp. 149–156, 2010.

[20] G. Meunier, B. Boulet, and M. Nahon, "Control of an overactuated cable-driven parallel mechanism for a radio telescope application," *IEEE Trans. Control Syst. Tech.*, vol. 17, no. 5, pp. 1043–1054, Sep. 2009.

[21] M. A. Khosravi and H. D. Taghirad, "Dynamic analysis and control of cable driven robots with elastic cables," *Trans. Can. Soc. Mech. Eng.*, vol. 35, no. 4, pp. 543–557, 2011.

[22] P. Kokotovic, H. K. Khalil, and J. O'Reilly, *Singular Perturbation Methods in Control: Analysis and Design*. New York, NY, USA: Academic, 1986.

[23] H. D. Taghirad and M. A. Khosravi, "Stability analysis and robust composite controller synthesis for flexible joint robots," *Adv. Robot.*, vol. 20, no. 2, pp. 181–211, 2006.

[24] C. Sui and M. Zhao, "Control of a 3-DOF parallel wire driven stiffness-variable manipulator," in *Proc. IEEE Int. Conf. Robot. Biomimet.*, 2004, pp. 204–209.

[25] A. Vafaei, M. A. Khosravi, and H. D. Taghirad, "Modeling and control of cable driven parallel manipulators with elastic cables: Singular perturbation theory," in *Proc. 4th Int. Conf. Intell. Robot. Appl.*, 2011, pp. 455–464.

[26] M. A. Khosravi and H. D. Taghirad, "Experimental performance of robust PID controller on a planar cable robot," in *Proc. 1st Int. Conf. Cable-Driven Parallel Robots*, 2012, pp. 337–352.

[27] M. Azadi, S. Behzadipour, and G. Faulkner, "Antagonistic variable stiffness elements," *Mech. Mach. Theory*, vol. 44, no. 9, pp. 1746–1758, 2009.

[28] S. Behzadipour and A. Khajepour, "Stiffness of cable-based parallel manipulators with application to stability analysis," *J. Mech. Design*, vol. 128, no. 1, pp. 303–310, 2006.

[29] S. Behzadipour and M. Azadi Sohi, "Antagonistic stiffness in cable-driven mechanisms," presented at the 12th IFToMM. World Congr., Besancon, France, 2007.

[30] A. Zarif and H. D. Taghirad, "Controllable workspace of cable-driven redundant parallel manipulators by fundamental wrench analysis," *Trans. Can. Soc. Mech. Eng.*, vol. 36, no. 3, pp. 297–314, 2012.

Mohammad A. Khosravi (M'13) received the B.Sc. degree in electrical engineering from the University of Sistan and Baluchistan, Zahedan, Iran, in 1997 and the M.Sc. and Ph.D. degrees in electrical engineering, both from K. N. Toosi University of Technology, Tehran, Iran, in 2000 and 2013, respectively.

He is currently with Advanced Robotics and Automated System, K. N. Toosi University of Technology. His current research interests include various aspects of dynamics and control of parallel robots with particular emphasis on cable-driven robots.

Hamid D. Taghirad (SM'12) received the B.Sc. degree in mechanical engineering from Sharif University of Technology, Tehran, Iran, in 1989 and the M.Sc. degree in mechanical engineering and the Ph.D. degree in electrical engineering from McGill University, Montreal, QC, Canada, in 1993 and 1997, respectively.

He is currently a Professor and the Dean of Faculty of Electrical Engineering, Department of Systems and Control and the Director of the Advanced Robotics and Automated System, K.N. Toosi University of Technology, Tehran. His publications include five books and more than 190 papers in international journals and conference proceedings. His research interests include robust and nonlinear control applied to robotic systems.

Dr. Taghirad is the Chairman of the IEEE control system chapter in the Iran section, a member of the board of the Industrial Control Center of Excellence, K. N. Toosi University of Technology. He is the Editor-in-Chief of Mechatronics Magazine and a member of the editorial board of *International Journal of Robotics: Theory and Application* and *International Journal of Advanced Robotic Systems*. His research interest includes robust and nonlinear control applied to robotic systems.